

Received August 19, 2017; reviewed; accepted April 1, 2018

## Investigations on soluble starch as the depressant of hematite during flotation separation of apatite

Shaojun Bai <sup>1,2</sup>, Zhan Ding <sup>1</sup>, Xianyu Fu <sup>1</sup>, Chunlong Li <sup>2</sup>, Chao Lv <sup>1,2</sup>, Shuming Wen <sup>1,2</sup>

<sup>1</sup> Faculty of Land Resources Engineering, Kunming University of Science and Technology, Kunming 650093, Yunnan, PR China

<sup>2</sup> State Key Laboratory of Complex Nonferrous Metal Resources Clean Utilization, Kunming 650093, Yunnan, PR China

Corresponding author: [shmwen@126.com](mailto:shmwen@126.com) (Shuming Wen), [2396418166@qq.com](mailto:2396418166@qq.com) (Chunlong Li)

**Abstract:** In this paper, soluble starch was studied as a depressant of hematite during flotation separation of apatite using sodium oleate as a collector. Surface charge measurement, soluble starch adsorptions, Fourier transform infrared spectroscopy (FTIR) and X-ray photoelectron spectroscopy (XPS) were used to understand the interaction mechanisms between minerals (hematite and apatite) and soluble starch. The results indicated that chemical interaction between hematite and soluble starch was present, and supported the bonding of hydroxyl, while physical adsorption of soluble starch molecules with apatite occurred. Results of micro-flotation studies suggested that soluble starch was considered as a selective depressant for hematite. The maximum recovery difference between hematite and apatite of 77.5% was obtained with 40 mg/dm<sup>3</sup> soluble starch. The flotation experiment results of natural iron ore showed that flotation indexes with 59.73% Fe, iron recovery of 81.5% and 75.68% of dephosphorization ratio were achieved at a soluble starch dosage of 60 mg/dm<sup>3</sup>. However, a higher dosage of soluble starch addition caused the difficulty for flotation separation of apatite from hematite. Our results provided theoretical basis for the flotation separation of apatite from iron oxide ores.

**Keywords:** soluble starch, depressant, hematite, apatite, FTIR, XPS

### 1. Introduction

In China, there is an urgent need to focus on utilizing domestic iron ore resources to mitigate risk of raw material shortage. However, characterization studies have indicated that most of the iron ore deposits in China have been exhibited an increasingly complex mineralogical composition and are either refractory or low-quality grade (Yong et al., 2010; Liu et al., 2013; Sun et al., 2015). For example, the deposits of high phosphorus hematite ores are widely spread, however, the chemical quality of the raw ore falls significantly below established industrial requirement and the minerals are liberated at extremely fine size. Thus, the main obstacle associated with exploiting these deposits is the fine dissemination of iron, silica, aluminum and phosphorus minerals, which affects the economy of iron making process. In fact, amongst these deleterious elements, the phosphorus, occurring primarily as apatite is an extremely harmful element in the steel making process, and causes detrimental effects on the product, such as increasing hardness and brittleness and decreasing ductility of the products (Nunes et al., 2012). Thus, the development of a successful and economic separation technique to remove apatite from the high phosphorus iron ores would significantly extend the reserves of phosphorus-content iron ores, and enhance the development of iron and steel industries (Fisher-White et al., 2012).

Reverse flotation, has been considered as one of the most widely utilized technology for high phosphorus iron ores separation (Araujo et al., 2005; Filippov et al., 2010; Ma et al., 2011). In reverse anionic flotation processing, the apatite is floated with fatty acids collectors after depressing the iron oxide by suitable reagents such as starch, dextrin, sodium silicate, and CMC. In addition, a series of studies have been undertaken to improve apatite separation efficiency, and also to develop novel

collectors to increase the floatability difference between apatite and other minerals (Cao et al., 2015; Liu et al., 2017; Jong et al., 2017; Quast, 2017). The results indicated that an effective depressant was essential for improving the floatability differences between valuable and gangue minerals. Amongst the above-mentioned depressing reagents, starch is the most widely used depressant of hematite due to its low cost and few negative impacts on the environment.

The depressant action of starch is due to the starch-hematite interaction, resulting in the coating of a natural low energy hydrophobic surface with a hydrophilic film or forming strong chemical complexes, and prevents the attachment of air bubbles and the collector from adsorbing onto hematite surfaces (Turrer and Peres, 2010). Weisborn et al. (1995) have indicated that the adsorptions of starch onto hematite surface are due to the availability of higher concentrations of hydroxylated metal sites based on the thermogravimetric analysis, infrared and zeta potential results. Ravishankar and Pradip (1995) have proposed the interaction of starch with iron oxide based on the basal plane and cleavage plane of iron oxides. Liu-yin et al. (2009) have suggested that hydrogen bonding is the underlying adsorption mechanism for starches with the oxide minerals. Recently, evidence has suggested that a chemical interaction between the polymer and hematite is the underlying adsorption mechanism for starches. Results reported by Somsook et al. (2005) have proposed the interaction between iron and polysaccharides based on several studies like TG-DTA, FTIR, EPR, NMR and TEM. Jain et al. (2012) have shown the interaction based on the electron density plot indicating the charge transfer between the Fe atom of hematite and the oxygen atom of starch. Although the depressant mechanisms of starch have been conducted by many researchers, most of them focus on the depressant of starch on the iron oxide minerals, and there is little literature on the effect of starch on the gangue minerals floatability, such as apatite, etc. Meanwhile, few researches were conducted so far concerning the XPS analysis of hematite and apatite surfaces treated with soluble starch. Actually, the investigation of both of the above analyses might be essential for understanding the interaction mechanisms between the starch and mineral surfaces, which have not yet been well established up to now.

In this paper, soluble starch has been studied as the depressant of hematite during flotation separation of apatite using sodium oleate as the collector. The interaction mechanism between the soluble starch and minerals (hematite and apatite) was studied with employment of Zeta-potential, Fourier Transform Infrared Spectroscopy (FTIR) and X-ray photoelectron spectroscopy (XPS). Our results might specify the interaction mechanisms between the starch and mineral surfaces and provide solidate theoretical basis for the flotation separation of apatite from iron oxide ores.

## 2. Experimental

### 2.1. Materials and reagents

High purity hematite and apatite used in the flotation studies were from Luoci dressing plant, affiliated in Kunming Iron And Steel Ltd, Yunnan, China, which were assaying 67.3% Fe (Total) and 40.85% P<sub>2</sub>O<sub>5</sub>, respectively. The natural occurring banded hematite and apatite (BHA) ore was also collected from Luoci dressing plant. X-ray diffraction pattern and chemical composition of raw materials are shown in Fig. 1 and Table 1, respectively. The finenesses of hematite and apatite were about 95% below 74 μm. The fineness of BHA was about 80% below 74 μm. Sodium hydroxide, soluble starch and sodium oleate (NaOl) with more than 98% purity were obtained from different chemical companies in China. Pure deionized water with a resistivity of 18 MU obtained from a Milli-Q50 system (Billerica, MA, USA) was used in all the experiments.

### 2.2. Materials and methods

#### 2.2.1. Flotation experiments

Pure mineral flotation experiments were carried out in a 50 cm<sup>3</sup> flotation cell (RK-FGC5, Wuhan) at 1800 rpm impeller speed. Mineral sample (2.0 g) was mixed with 40 cm<sup>3</sup> od deionized water in flotation cell for 1 min (Gao et al. 2016a, b; Wang et al., 2017). Meanwhile, the BHA flotation experiments were carried out in 1500 cm<sup>3</sup> flotation cell (XFD-63, Wuhan) Li and Gao, 2017; Gao et al., 2018). NaOH were added in the pulp for pH adjustment, and the pulp was conditioned for 2 min. Soluble starch and sodium oleate (NaOl) were then separately added, and the pulp was conditioned for 2 min with each reagent addition.

The flotation time was fixed for 5 min at room temperature (25°C). Recovery of the flotation products, Fe grade, P-content and dephosphorization ratio were determined and treated as the indexes to evaluate the flotation effects. The dephosphorization ratio (DR) was calculated by the following equation:

$$DR = 1 - \frac{\beta}{\alpha} \gamma \times 100\% \quad (1)$$

where DR is the dephosphorization ratio of sink product;  $\beta$  is the p-content in sink product;  $\alpha$  is the p-content in BHA ore and  $\gamma$  is the yield of sink product.

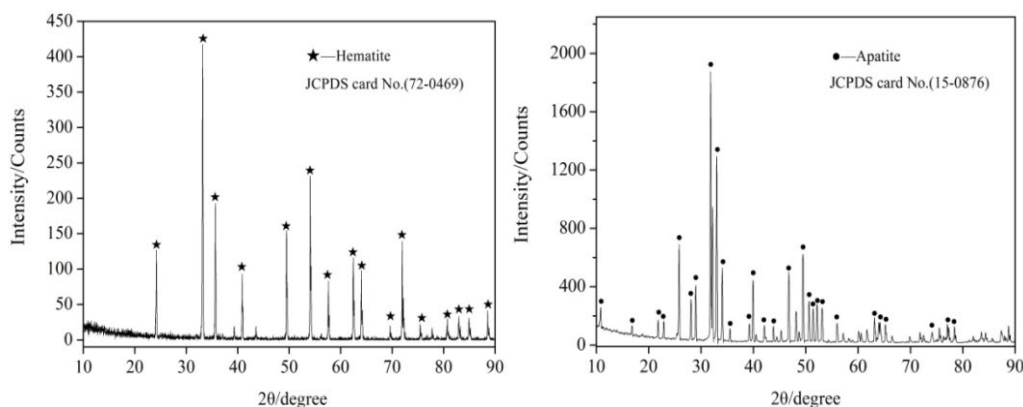


Fig. 1. X-ray diffraction pattern of the materials

Table 1. Chemical composition of raw materials (wt.%)

Material	Fe <sub>2</sub> O <sub>3</sub>	Al <sub>2</sub> O <sub>5</sub>	CaO	MgO	SiO <sub>2</sub>	P <sub>2</sub> O <sub>5</sub>	LOI
Hematite	96.15	<0.5	0.56	0.14	0.49	0.49	0.41
Apatite	0.59	<0.05	52.26	<0.005	1.25	40.85	0.53
BHA	80.05	1.09	3.82	3.10	14.85	2.27	0.48

### 2.2.2. Adsorption test

Ultraviolet spectrophotometry was performed to measure the amount of soluble starch adsorption on the sample surfaces. 2.0 g of mineral sample was mixed with 35 mL of deionized water in a 50 mL volumetric flask for 2 min. NaOH was added to maintain the pH at about 10. Afterward, different dosage soluble starch was added to the flask respectively and thus the initial concentration in the solution ranged from 10 mg/dm<sup>3</sup> to 80 mg/dm<sup>3</sup>. Then, the flask was placed in a mechanical shaker at room temperature for 30 min for a complete adsorption. Finally, the suspension of minerals was centrifuged and the supernatant was taken out for determination of soluble starch concentration by using a UV-Visible spectrophotometer (UV765, Shanghai) with a wave length of 490 nm. The amount of soluble starch adsorbed on each sample was calculated by the following equation:

$$\Gamma = \frac{(c_0 - c_t)}{m} v \quad (2)$$

where  $\Gamma$  is the adsorption amount (mg g<sup>-1</sup>);  $C_0$  is the initial concentration of soluble starch in the solution (mg/dm<sup>3</sup>);  $C_t$  is the residual concentration of soluble starch in the supernatant (mg/dm<sup>3</sup>);  $v$  is the supernatant volume (dm<sup>3</sup>), and  $m$  is the sample weight (g).

### 2.2.3. Zeta potential measurements

Zeta-potential study of the samples before and after interacting with soluble starch was measured using the zeta probe analyzer (Zetesizer-3000HS, Malvem Instrument Ltd). All the samples were thoroughly equilibrated, and the measurements were recorded in a dilute suspension of 1% solids by weight. Zeta potentials of the samples were recorded through artificial determination at different pH conditions.

### 2.2.4. FTIR measurements

FTIR spectrometer (Tensor, Bruker) was used to determine the interactions that might occur between reagents and minerals. Pure minerals were ground to  $-2\ \mu\text{m}$  in an agate mortar and then conditioned with soluble starch in a laboratory stirrer for 30 min at about  $\text{pH}=10$ . In order to verify the nature of soluble starch adsorbed in the pure minerals, the concentration of the reagents used in the FTIR study was twenty times as much as that used in pure mineral flotation experiments. At the end, the fully interacted samples were separated by filtration, thoroughly rinsed with the corresponding pH solution and dried at room temperature.

### 2.2.5. X-ray photoelectron spectroscopy (XPS) analysis

A 2.0 g of the pure mineral was conditioned with  $40\ \text{mg}/\text{dm}^3$  soluble starch in a laboratory stirrer for 30 min at about  $\text{pH}=10$ . The fully interacted samples were separated by filtration, thoroughly rinsed with the corresponding pH solution and dried at room temperature for XPS analysis. The dry product was examined using a PHI5000 Versa Probe II (PHI5000, ULVAC-PHI, Japan) with an Al Ka X-ray source. The MultiPak Spectrum software was used to calculate and analyze the spectra and surface atomic ratios of the measured samples. The C1s spectral peak at 284.8 eV was obtained to calibrate all of the measured spectra as an internal standard for charge compensation.

## 3. Results and discussion

### 3.1. Flotation of samples

#### 3.1.1. Effect of soluble starch dosage

Experiments are carried out on the floatability of apatite in the presence of the collector NaOl ( $4 \times 10^{-4}\ \text{mol}/\text{dm}^3$ ) and solution pH at 10 on basis of experiment results as a function of soluble starch dosage. The results are shown in Fig. 2. It is observed that soluble starch exhibits a depression effect on hematite and apatite flotation recovery. Furthermore, this depression on hematite is more obvious than the depression on apatite with the increase of soluble starch dosage. When the soluble starch dosage was  $0\ \text{mg}/\text{dm}^3$ , the recovery difference between hematite and apatite is about 56.8%. This indicates that the hematite and apatite are floated by NaOl, and it is difficult to selectively separate the two minerals in the absence of soluble starch. A max recovery difference between hematite and apatite of 77.5% is obtained with  $40\ \text{mg}/\text{dm}^3$  soluble starch dosage addition. With a further increase in the soluble starch dosage from 40 to  $80\ \text{mg}/\text{dm}^3$ , the change in the hematite recovery is negligible, but a sharp decrease in the apatite recovery is present. These results demonstrate that the soluble starch interact with apatite, inclusive the soluble starch-hematite interaction. Moreover, the physicochemical difference between hematite and apatite decreases obviously with vast soluble starch addition (more than  $40\ \text{mg}/\text{dm}^3$ ). Therefore, the selective flotation separation between the two minerals can be reinforced in the presence of an appropriate soluble starch dosage.

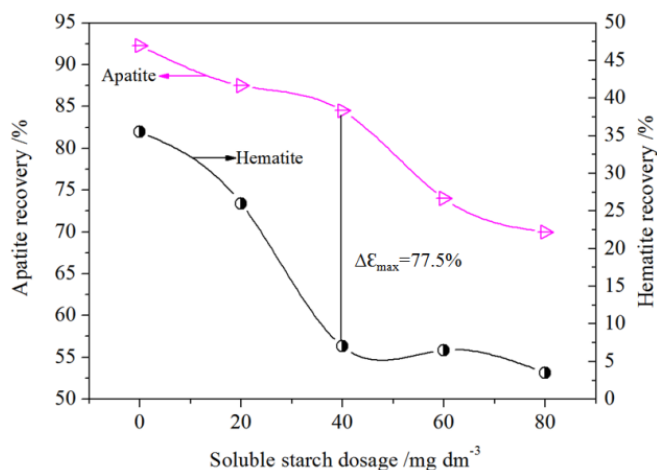


Fig. 2. The flotation of hematite and apatite at different soluble starch dosage

### 3.1.2. Flotation of BHA ore

One aim of this investigation is to realize apatite removal from the banded hematite and apatite (BHA) ore. Fig. 3 presents the influence of different soluble starch dosage on the flotation of BHA ore with the NaOH dosage fixed at  $4 \times 10^{-4}$  mol/dm<sup>3</sup> and solution pH at 10. As evident from the figure Fig. 3 (a), the soluble starch acts as the depressant of the hematite. The Fe grade in sink product and Fe recovery increase when the soluble starch dosage increases from 0 mg/dm<sup>3</sup> to 60 mg/dm<sup>3</sup>. However, with a further increase in soluble starch dosage, the grade of iron starts decreasing, while the iron recovery does not increase significantly. This phenomenon may attribute to the depression of gangue minerals on the condition of a higher dosage of soluble starch. The findings are consistent with the observations reported by Kar et al. (2013), Pavlovic and Brandao (2003). Fig. 3 (b) shows that the dephosphorization ratio decreases, and the p-content in sink product rises due to the increase of soluble starch dosage. That is, it is possible to recover 81.5% of iron values and remove 75.68% of phosphorus at a soluble starch dosage of 60 mg/dm<sup>3</sup>. Moreover, the iron grade of BHA can be increased by 3.41% comparing with the corresponding flotation indexes at a soluble starch dosage of 0 mg/dm<sup>3</sup>. However, obvious deterioration in flotation indexes is observed when the soluble starch dosage is 80 mg/dm<sup>3</sup>. This indicates that the soluble starch interacts with apatite, depressing the apatite. The depression behavior is more evident when a higher dosage of soluble starch is added, resulting in the difficulty for apatite removal from the BHA ore. Importantly, the above results are well agreed with the flotation results of pure minerals.

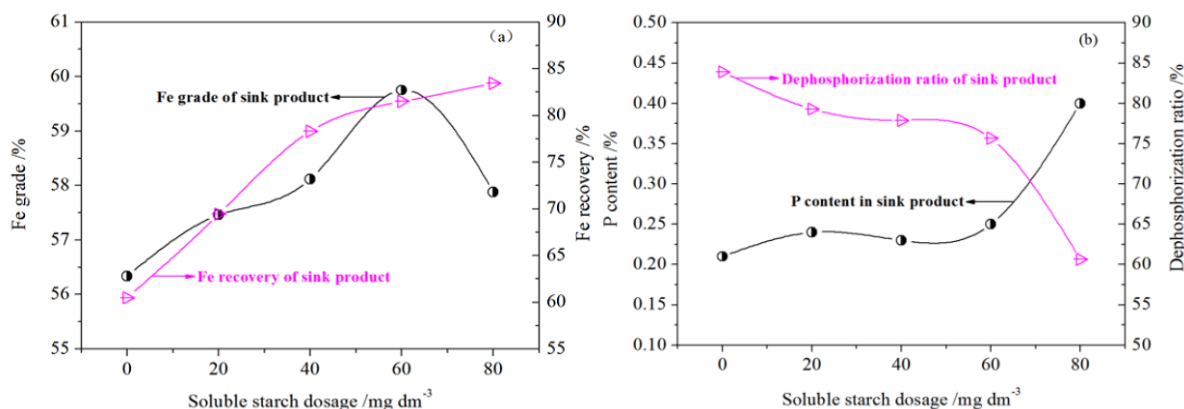


Fig. 3. The flotation of BHA ore at different soluble starch dosage

### 3.2. Zeta potential determination

The effect of soluble starch on the zeta potential of hematite and apatite is presented in Fig.4. The results indicate that the iso-electric point of hematite is at pH 5.82 in the absence of soluble starch, which is in good agreement with the previous report (Montes and Atenas, 2005). Furthermore, it has an evident decrease in the zeta potential of hematite by the addition of 40 mg/dm<sup>3</sup> soluble starch [Fig.4 (a)]. Thus, the adsorption of soluble starch has affected the surface potential of hematite, which might be explained in terms of chemisorption of hydroxyl ions (active hydroxyl sites) on the surface of hematite surfaces (Pavlovic and Brandao, 2003). The isoelectric point (IEP) of apatite was not observed when pH range from 4.6 to 13. It has a negligible shift on the zeta potential of apatite with the addition of 40 mg/dm<sup>3</sup> soluble starch [Fig.4 (b)], that is, the zeta potential decreases by 0.99 mV and 1.23 mV, respectively, when the pH value is 9.8 and 11.5, which may be due to the physical adsorption on apatite surfaces. Based on the results of zeta potential determination, the addition of soluble starch will therefore benefit for the flotation separation of apatite from hematite; it was also well verified by the flotation results of pure minerals.

The results of adsorption amount of soluble starch on hematite and apatite are shown in Fig. 5. As can be seen, the adsorption amount on two minerals increases with the increase of the initial concentration of soluble starch, and the adsorption amount of soluble starch on hematite is higher than that on apatite. These results are consistent with the work of Filippov et al. (2013), Tang and Wen (2015). From Fig.5, it is evident that there is a corresponding increase in adsorption amount when the soluble

starch initial concentration increases up to 60 mg/dm<sup>3</sup>. In this case, the adsorption isotherms are considered to be of a linear shape. Additionally, clear plateaus of adsorption amount (0.38 mg g<sup>-1</sup> for hematite and 0.15 mg g<sup>-1</sup> for apatite) are observed for hematite and apatite at initial concentrations above 60 mg/dm<sup>3</sup> of soluble starch. This result can be well explained by Khosla and Biswas's (1984) theory, which indicates that free starch molecules might be adsorbed at the active sites of the mineral surface until saturation. It can be concluded that the depression performance of hematite can be reasonably correlated with that of the amount of soluble starch adsorbed, and such correlation have been also observed on the floatability of apatite. Merely, this depression performance for apatite is not obvious on the condition of low concentration soluble starch addition.

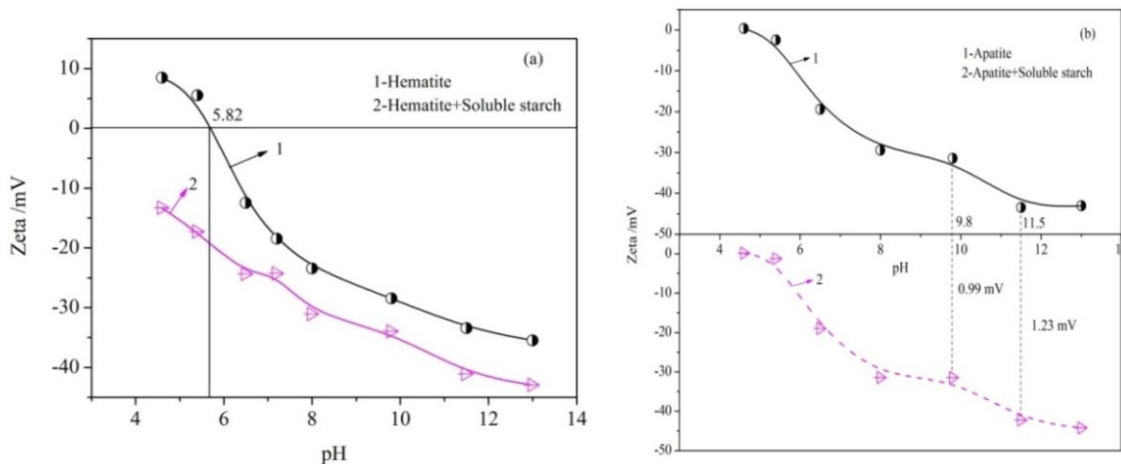


Fig. 4. Zeta-potential of sample as a function of pH by the addition of soluble starch for: (a) hematite, (b) apatite

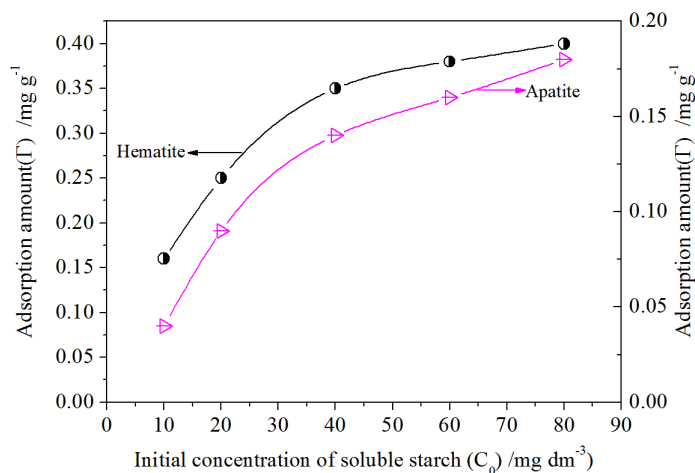


Fig. 5. The effect of soluble starch initial concentration on adsorption amount on hematite and apatite at pH 10

### 3.3. FTIR analysis

FTIR spectra of hematite and apatite before and after reaction with soluble starch are shown in Fig. 6. Fig. 6 (A-a) shows that the adsorption bands in 3443.63 cm<sup>-1</sup> and 2918.01 cm<sup>-1</sup> are due to OH and CH stretching, respectively (Yan and Zhang, 2011). The observed frequency at 1644.61 cm<sup>-1</sup> is related to the vibration of bound water molecules. This water band is dependent on the number of water molecules associated with the starch molecules (Heyn, 1974). The band located at 1459.05 cm<sup>-1</sup> and 857.01 cm<sup>-1</sup> are due to plane bending and vibrations associated with the CH<sub>2</sub> group, while the band at 1374.05 cm<sup>-1</sup> corresponds to C-OH vibration (Pawlak and Mucha, 2003). The C-O-C stretch contributes to modes related to the bands at 1158.74 cm<sup>-1</sup>. Intense bands observed at 1085.08 cm<sup>-1</sup> and 991.59 cm<sup>-1</sup> are attributed to C-O stretch. The modes related with C-OH ring vibration were identified at 929.63 cm<sup>-1</sup>, 764.95 cm<sup>-1</sup>, 575.12 cm<sup>-1</sup> and 525.54 cm<sup>-1</sup> (Cael et al., 1975).

The characteristic peak of hematite appears at 1037.33 cm<sup>-1</sup> due to Fe-O bonding [Fig. 6 (A-b)]. Other

peaks at  $3441.08\text{ cm}^{-1}$  and  $1638.94\text{ cm}^{-1}$  correspond to the stretching vibration of OH groups and bending vibration of water molecules respectively, which indicates the presence of OH groups and water molecules in hematite (Venjaminov and Prendergast, 1997; Gao et al., 2017). Fig. 6 (A-c) shows the infrared spectra of soluble starch interacted with hematite. The characteristic hematite peak of  $1037.33\text{ cm}^{-1}$  has shifted to  $1045.16\text{ cm}^{-1}$ , and the OH stretching bands of soluble starch is shifted by  $32.4\text{ cm}^{-1}$ . This indicates the involvement of OH groups of soluble starch in the adsorption on hematite. Furthermore, appearance of the new bands at  $2977.59\text{ cm}^{-1}$ ,  $2908.17\text{ cm}^{-1}$  and  $1453.38\text{ cm}^{-1}$  are observed due to CH stretching in soluble starch, while new band at  $1398.13\text{ cm}^{-1}$  are attributed to C-OH vibration, indicating the chemical adsorption of soluble starch molecules with hematite (You et al., 2009). The spectra [Fig. 6 (B)] are very similar indicating that the observed frequencies arise from similar vibrational modes. The primary differences between the blank apatite infrared spectrum and the spectrum of apatite treated with soluble starch include the appearance of new bands at  $2979.00\text{ cm}^{-1}$  and  $2905.34\text{ cm}^{-1}$ , which is due to CH stretching in soluble starch. Thus, the locations of characteristic peaks of apatite do not have any shift. Merely, the intensity of characteristic peaks changes. We infer that the physical adsorption of soluble starch molecules with apatite occurs.

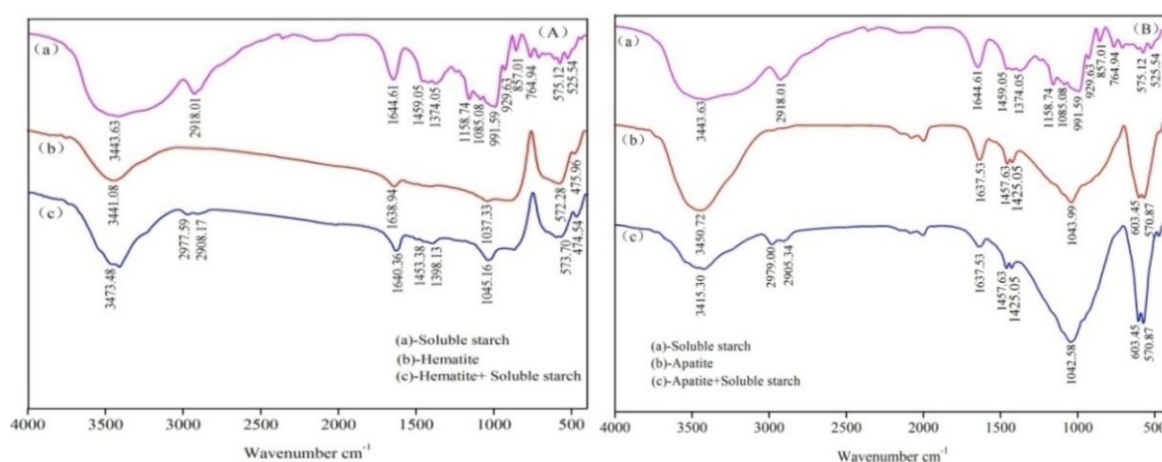


Fig. 6. (A) Infrared spectra for soluble starch adsorbed on hematite and (B) Infrared spectra for soluble starch adsorbed on apatite

### 3.4. XPS studies

The XPS technique can determine the chemical states of elements, which is valuable to analyze the adsorption phenomena on mineral surface. Table 2 shows the XPS characterization of hematite before and after interacting with  $40\text{ mg/dm}^3$  soluble starch at pH 10. Adsorption of the soluble starch on hematite manifests in the XPS spectra by an increase in atomic concentration of the C and a decrease in atomic concentration of O and Fe, respectively, comparing with that of the initial hematite surface (Table 2).

Table 2. XPS characterization of hematite before and after interacting with soluble starch

Samples	Assignments	C1s	O1s	O2s	O KLL	Fe2p	Fe3p	Fe3s	Fe LMM
Hematite	Binding Energy/eV	284.80	531.38	5.06	960~1000	711.86 725.73	23.79	56.70	770~920
	Atomic Concentration/%	38.72		52.05			9.23		
Hematite+ Soluble starch	Binding Energy/eV	284.80	531.96	6.77	960~1000	711.92 725.49	24.34	56.92	770~920
	Atomic Concentration/%	42.57		50.36			7.06		

The O1s and Fe2p XPS spectra and the fitting curves of hematite before and after interacting with soluble starch are shown in Figs. 7 and 8. As shown in Fig. 7 (a), the main peak at approximately 531.20 eV is assigned to the oxygen in O-H bond. The O1s spectrum contains the peaks at approximately 529.99 eV, corresponding to oxygen in the Fe<sub>2</sub>O<sub>3</sub>, and at approximately 532.49 eV, which is assigned to C-O bond. Significant changes in the BE and FWHM values of O1s peak for hematite after interacting with soluble starch are observed in Fig. 7 (b) comparing with that of untreated hematite [Fig. 7 (a)]. The O1s is fitted into four components, and the fitted component at a binding energy of 533.70 eV and new FWHM values of 1.08 eV presented is related to the O-C-O linkage. Moreover, From Table 2, the binding energy (531.96 eV) of the O1s spectra of the hematite after interacting with soluble starch is higher than that of the untreated hematite (531.38 eV) because of the modification of their chemical environment, which indicates the adsorption of soluble starch molecules with hematite.

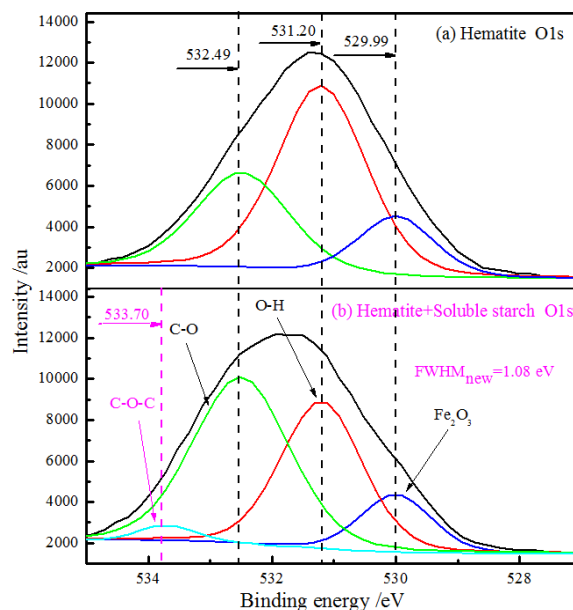


Fig. 7. O1s XPS spectra and the fitting curves of hematite before and after interacting with soluble starch

Fig. 8 shows Fe 2p and Ca2p XPS spectra of the samples before and after interacting with 40 mg/dm<sup>3</sup> soluble starch at pH 10. According to the studies of Omran et al. (2015) and Hu et al. (2016), the Fe 2p<sub>1/2</sub> and Fe 2p<sub>3/2</sub> envelopes are fitted using peaks corresponding to the multiplets, surface structures, shake-up satellites and pre-peak. For hematite [Fig. 8 (a)], the Fe 2p spectrum contains two peaks of Fe 2p<sub>3/2</sub> and Fe 2p<sub>1/2</sub> at binding energy (B.E.) positions of 711.86 eV and 725.73 eV, respectively. The observed signals at these B.E. positions seem to correspond to the Fe<sup>3+</sup> in Fe<sub>2</sub>O<sub>3</sub> (hematite) phase (Wagner et al., 1979; Roosendaal et al., 1999). The Fe 2p<sub>3/2</sub> peak has associated satellite peaks at 719.70 eV. Researchers have investigated that the satellite peak of Fe 2p<sub>3/2</sub> for Fe<sub>2</sub>O<sub>3</sub> is located approximately 8 eV higher than the main Fe 2p<sub>3/2</sub> peak (Nasibulin et al., 2009; Yuan et al., 2012). This conclusion is supported by present Fe 2p XPS spectra results. The observed B.E. difference between Fe 2p doublet spectra, i.e., between Fe 2p<sub>3/2</sub> and Fe 2p<sub>1/2</sub> is 13.87 eV corresponding to hematite phase. For hematite after interacting with soluble starch [Fig.8 (b)], there is a significant shift in the position of the peak maxima in the Fe 2p doublet, the B.E. positions are observed to be at 711.92 eV for Fe 2p<sub>3/2</sub> and 725.49 eV for Fe 2p<sub>1/2</sub>, and the observed B.E. difference is 13.57 eV, which decreased by 0.3 eV comparing with the result of untreated hematite. In addition, the fitted component at a binding energy of 711.15 eV and a new FWHM value of 1.57 eV, is related to the FeOOH (Moulder et al., 1992), which indicates the chemical adsorption of soluble starch on hematite surface.

As shown in Fig. 8 (c), the Ca 2p spectrum of apatite sample in absence of soluble starch contains two peaks of Ca 2p<sub>1/2</sub> and Ca 2p<sub>3/2</sub> at binding energy (B.E.) positions of 350.77 eV and 347.23 eV, respectively (Jong et al., 2017). The observed B. E. difference between Ca 2p doublet spectra is 3.54 eV. The XPS spectra of apatite sample after treatment of soluble starch is presented in Fig. 8 (d). Two peaks at 350.80 eV, and 347.25 eV are found in Ca 2p<sub>1/2</sub> and Ca 2p<sub>3/2</sub> emission of apatite sample and the

observed B.E. difference is 3.55 eV. On basis of the negligible changes in the binding energy of Ca2p, we inferred that chemical adsorption of soluble starch did not occur at Ca sites on the apatite surface.

Thus, XPS studies demonstrated that interaction mechanism between the soluble starch and hematite occurs via the hydroxyl groups attached to the C atoms from the adjacent glucopyranose rings of the soluble starch molecules reacting with the surface iron atoms of hematite, resulting in the depressing activity of hematite. Additionally, the chemical interaction between the soluble starch and the apatite are negligible when a 40 mg/dm<sup>3</sup> of soluble starch is added. In fact, there are four OH groups available on the soluble starch molecules. However, the OH groups closer to the heterocyclic oxygen are more polarisable compared to other OH groups. The lone pair of electrons on oxygen atoms present in polarisable oxygen atoms will interact with the vacant d-orbitals available on Fe atoms of iron oxide.

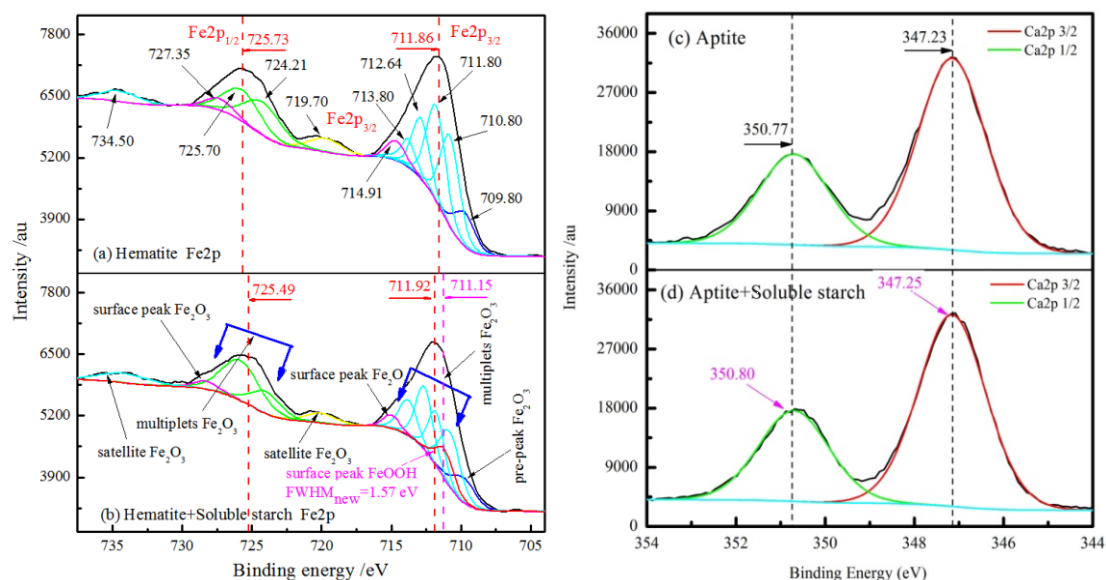


Fig. 8. Fe 2p and Ca2p XPS spectra of the samples before and after interacting with soluble starch

#### 4. Conclusions

Experimental research indicates that hematite is depressed obviously and apatite can be floated well when soluble starch is used as the depressant of the anion reverse flotation separation between the hematite and the apatite with the employment of sodium oleate (NaOl) collector at a pulp pH of 10. The flotation studies have indicated that the apatite has a better floatability than that of the hematite. The max recovery difference between hematite and apatite of 77.5% is obtained with 40 mg/dm<sup>3</sup> soluble starch dosage addition. The flotation of natural iron ore indicates that flotation indexes with 59.73% Fe, iron recovery of 81.5% and 75.68% of dephosphorization ratio can be achieved at a soluble starch dosage of 60 mg/dm<sup>3</sup>. However, a higher dosage of soluble starch causes the difficulty for apatite removal from hematite. The major changes in the FTIR and XPS spectra of hematite suggest the presence of chemical interaction between hematite and soluble starch, and support the bonding of hydroxyl. The above-mentioned results are also supported by the zeta-potential measurement and adsorption amount of soluble starch. Results of XPS, FTIR, zeta potential and soluble starch adsorptions have indicated that the apatite-soluble starch interaction occurs, and support physical adsorption of soluble starch molecules with apatite. The physicochemical difference between hematite and apatite will increase with low concentration soluble starch addition. This is very important for the selective flotation separation of apatite from hematite.

#### Acknowledgements

The authors would like to express their gratitude for the financial support from the National Natural Science Foundation of China (Grant No. 51664027) and National Science Foundation for Young Scientists of China (Grant No.51404118) and the authors are grateful to the Analysis and Testing Centre in Kunming University of Science and Technology for its technical support (2016T20110055).

## References

- ARAUJO, A.C., VIANA, P.R.M., PERES, A.E.C., 2005. *Reagents in iron ores flotation*. Minerals Engineering, 18, 219-224.
- CAEL, J.J., KOENIG, J.L., BLACKWELL, J., 1975. *Infrared and Raman spectroscopy of carbohydrates. Part VI: normal coordinate analysis of V-amylose*. Biopolymers, 14, 1885-1903.
- CAO, Q., CHENG, J., WEN, S., LI, C., BAI, S., LIU, D., 2015. *A mixed collector system for phosphate flotation*. Minerals Engineering, 78, 114-121
- FILIPPOV, L.O., FILIPPOVA, I.V., SEVEROV, V.V., 2010. *The use of collectors mixture in the reverse cationic flotation of magnetite ore: The role of Fe-bearing silicates*. Minerals Engineering, 23, 91-98.
- FILIPPOV, L.O., SEVEROV, V.V., FILIPPOVA, I.V., 2013. *Mechanism of starch adsorption on Fe-Mg-Al-bearing amphiboles*. Int J Miner Process, 123, 120-128.
- FISHER-WHITE, M.J., LOVEL, R.R., SPARROW, G.J., 2012. *Heat and Acid Leach Treatments to Lower Phosphorus Levels in Goethitic Iron Ores*. Isij Int, 52, 1794-1800.
- GAO, Y.S., GAO, Z.Y., SUN, W., YIN, Z.G., WANG, J.J., HU Y.H., 2018. *Adsorption of a novel reagent scheme on scheelite and calcite causing an effective flotation separation*. J Colloid Interface Sci, 512, 39-46.
- GAO, Z.Y., LI, C.W., SUN, W., HU, Y.H., 2017. *Anisotropic surface properties of calcite: A consideration of surface broken bonds*. Colloid Surface A, 520, 53-61.
- GAO, Y.S., GAO, Z.Y., SUN, W., HU, Y.H., 2016 a. *Selective flotation of scheelite from calcite: A novel reagent scheme*, International Journal of Mineral Processing, 154, 10-15.
- GAO, Z.Y., GAO, Y.S., ZHU, Y.Y., HU, Y.H., SUN, W., 2016 b. *Selective flotation of calcite from fluorite: a novel reagent schedule*. Minerals, 6 (4), 114.
- HEYN, A.N.J., 1974. *The infrared absorption spectrum of dextran and its bound water*. Biopolymers, 13, 475-506.
- HU, H.P., WANG, M., DING, Z.Y., JI, G.F., 2016. *FT-IR, XPS and DFT Study of the Adsorption Mechanism of Sodium Salicylate onto Goethite or Hematite*. Acta Phys-Chim Sin, 32, 2059-2068.
- JAIN, V., RAI, B., WAGHMARE, U.V., PRADIP, 2012. *Molecular modeling based selection and design of selective reagents for beneficiation of alumina rich iron ore slimes*. Proceedings XXVI International Mineral Processing Congress, New Delhi, India, pp. 2258-2269.
- JONG, K., HAN, Y., RYOM, S., 2017. *Flotation mechanism of oleic acid amide on apatite*. Colloid Surface A, 523, 127-131.
- KAR, B., SAHOO, H., RATH, S.S., DAS, B., 2013. *Investigations on different starches as depressants for iron ore flotation*. Miner Eng, 49, 1-6.
- KHOSLA N.K., BHAGAT, R.P., GANDHI, K.S., BISWAS, A.K., 1984. *Calorimetric and other interaction studies on mineral-starch adsorption systems*. Colloids Surf, 8, 321-335.
- LI, C., GAO Z., 2017. *Effect of grinding media on the surface property and flotation behavior of scheelite particles*. Powder Technol, 322, 386-392.
- LIU-YIN, X., ZHONG, H., LIU, G.Y., WANG, S., 2009. *Utilization of soluble starch as a depressant for the reverse flotation of diasporite from kaolinite*. Miner Eng, 22, 560-565.
- LIU, S.Q., ZHANG, M., WANG, W.P., LI, X.J., 2013. *A Combined Beneficiation Process to Recover Iron Minerals from a Finely Disseminated Low-Grade Iron Ore*. Advances in Chemical, Material and Metallurgical Engineering, Pts 1-5 634-638, 3273-3276.
- LIU, X., RUAN, Y.Y., LI, C.X., CHENG, R.J., 2017. *Effect and mechanism of phosphoric acid in the apatite/dolomite flotation system*. International Journal of Mineral Processing, 167, 95-102.
- MA, X., MARQUES, M., GONTIJO, C., 2011. *Comparative studies of reverse cationic/anionic flotation of Vale iron ore*. International Journal of Mineral Processing, 100, 179-183.
- MOULDER, J.F., STICKLE, W.F., SOBOL, P.E., BOMBEN, K.D., CHASTAIN, J., 1992. *Handbook of X-ray Photoelectron Spectroscopy*. Eden Prairie, Perkin-Elmer Corporation, p. 439.
- NASIBULIN, A.G., RACKAUSKAS, S., JIANG, H., TIAN, Y., MUDIMELA, P.R., SHANDAKOV, S.D., NASIBULINA, L.I., SAINIO, J., KAUPPINEN, E.I., 2009. *Simple and Rapid Synthesis of alpha-Fe<sub>2</sub>O<sub>3</sub> Nanowires Under Ambient Conditions*. Nano Res, 2, 373-379.
- NUNES, A.P.L., PINTO, C.L.L., VALADAO, G.E.S., VIANA, P.R.D., 2012. *Floatability studies of wavellite and preliminary results on phosphorus removal from a Brazilian iron ore by froth flotation*. Miner Eng, 39, 206-212.
- OMRAN, M., FABRITIUS, T., ELMANDY, A.M., ABDEL-KHALEK, N.A., EL-AREF, M., ELMANAWI, A., 2015. *XPS and FTIR spectroscopic study on microwave treated high phosphorus iron ore*. Appl Surf Sci, 345, 127-140.
- PAVLOVIC, S., BRANDAO, P.R.G., 2003. *Adsorption of starch, amylose, amylopectin and glucose monomer and their effect*

- on the flotation of hematite and quartz. *Miner Eng*, 16, 1117-1122.
- PAWLAK, A., MUCHA, A., 2003. *Thermogravimetric and FTIR studies of chitosan blends*. *Thermochim Acta*, 396, 153-166.
- QUAST, K., 2017. *Literature review on the use of natural products in the flotation of iron oxide ores*. *Miner Eng*, 108, 12-24.
- RAVISHANKAR, S.A., PRADIP, K., N.K., 1995. *Selective flocculation of iron oxide from its synthetic mixtures with clays: a comparison of polyacrylic acid and its starch polymers*. *Int J Miner Process*, 43, 235-247.
- ROOSENDAAL, S.J., VAN ASSELE, B., ELSENAAR, J.W., VREDENBERG, A.M., HABRAKEN, F.H.P.M., 1999. *The oxidation state of Fe(100) after initial oxidation in O<sub>2</sub>*. *Surf Sci Rep*, 44, 329-337.
- SOMSOOK, E., HINSIN, D., BUAKHRONG, P., TEANCHAI, R., MOPHAN, N., POHMAKOTR, M., SHIOWATANA, J., 2005. *Interactions between iron(III) and sucrose, dextran, or starch in complexes*. *Carbohydr Polym*, 61, 281-287.
- SUN, Y.S., HAN, Y.X., GAO, P., WEI, X.C., LI, G.F., 2015. *Thermogravimetric study of coal-based reduction of oolitic iron ore: Kinetics and mechanisms*. *Int J Miner Process*, 143, 87-97.
- TANG, M., WEN, S.M., 2015. *Flocculation/Dispersion of Hematite with Caustic Digested Starch*. *Physicochemical Problems of Mineral Processing*, 51, 477-489.
- TIAN, M., GAO, Z., HAN, H., SUN, W., HU, Y., 2017. *Improved flotation separation of cassiterite from calcite using a mixture of lead (II) ion / benzohydroxamic acid as collector and carboxymethyl cellulose as depressant*. *Miner Eng*, 113, 68-70.
- TURRER, H.D.G., PERES, A.E.C., 2010. *Investigation on alternative depressants for iron ore flotation*. *Miner Eng*, 23, 1066-1069.
- VENYAMINOV, S.Y., PRENDERGAST, F.G., 1997. *Water (H<sub>2</sub>O and D<sub>2</sub>O) molar absorptivity in the 1000-4000 cm<sup>-1</sup> range and quantitative infrared spectroscopy of aqueous solutions*. *Analytical Biochemistry*, 248, 234-245.
- WANG J., GAO Z., GAO Y., HU Y., SUN W, 2017. *Flotation separation of scheelite from calcite using mixed cationic/anionic collectors*. *Miner Eng*, 98, 261-263.
- WAGNER, C.D., GALE, L.H., RAYMOND, R.H., 1979. *Two-dimensional chemical state plots: a standardized data set for use in identifying chemical states by x-ray photoelectron spectroscopy*. *Anal. Chem.*, 51, 466-482.
- YAN, H.J., ZHANG, B.S., 2011. *In vitro cytotoxicity of monodispersed hematite nanoparticles on Hek 293 cells*. *Mater Lett*, 65, 815-817.
- YONG, W.H., ZHANG, Y.S., GONG, W.Q., 2010. *Process Mineralogy and Mineral Processing Technology of Colloid Sedimentary Iron Ore*. *Regulatory Regional Economic Challenge for Mining, Investment, Environment and Work Safety*, 49-55.
- YOU, L.J., LU, F.F., LI, D., QIAO, Z.M., YIN, Y.P., 2009. *Preparation and flocculation properties of cationic starch/chitosan crosslinking-copolymer*. *J Hazard Mater*, 172, 38-45.
- YUAN, L., WANG, Y.Q., CAI, R.S., JIANG, Q.K., WANG, J.B., LI, B.Q., SHARMA, A., ZHOU, G.W., 2012. *The origin of hematite nanowire growth during the thermal oxidation of iron*. *Mater Sci Eng B-Adv*, 177, 327-336.